

# ✂ Evidence of Two $\beta'$ Phases in Tristearin

T.D. SIMPSON and J.W. HAGEMANN, Northern Regional Research Center, Agricultural Research, Science and Education Administration, U.S. Department of Agriculture, Peoria, IL 61604

## ABSTRACT

Data from Raman spectroscopy, X-ray diffraction analysis, differential scanning calorimetry and features of the preparative method are all consistent with the existence of 2 intermediate  $\beta'$  phases for tristearin; the first, a lower melting phase,  $\beta'_2$ , transforms at 61 C into the second,  $\beta'_1$ , which in turn changes at 64 C into  $\beta$ -tristearin. Raman spectral evidence indicates that the 2 mesophases occur in an orthorhombic packing environment and that the  $\beta'_2$  to  $\beta'_1$  transition results from a change in lateral packing of the hydrocarbon chains.

## INTRODUCTION

Polymorphism of solid triglycerides has long been a subject of controversy and attempted reconciliation (1-7). The existence or nonexistence and identifying characteristics of multiple intermediate states have remained uncertain even though there have been reports of several  $\beta'$  intermediate states for tristearin and tristearin dominant mixtures such as cocoa butter (6,8). The work presented here addresses particularly questions of the existence of the  $\beta'_1$  form observed by Hagemann et al. (6) using differential scanning calorimetry (DSC).

## MATERIALS AND METHODS

Tristearin was purchased as a white crystalline powder from Nu-Chek-Prep, Inc., Elysian, MN. Purity of the compound was checked as greater than 99% as determined by gas chromatography (GC) of the constituent acids as methyl esters. No further purification was performed.

Raman spectra were taken with a Spex Ramalab Model RS-2 spectrometer equipped with a RCA C-31034 photomultiplier and a Spectra-Physics 165-08 Argon laser. Samples in sealed 0.9-mm Kimax<sup>®</sup> glass capillaries were illuminated with 150 mW of 514.5 nm radiation. Spectral resolution was of the order of 4  $\text{cm}^{-1}$ . Spectra were calibrated vs the spectrum of indene, rendering a spectral frequency resolution of  $\pm 3 \text{ cm}^{-1}$ . Scan rate was 50  $\text{cm}^{-1}/\text{min}$ . Spectra were taken at subzero temperatures using a Spex Harney-Miller variable temperature assembly. A thermistor incorporated into the assembly was used to monitor the temperature.

X-ray powder diffraction data were taken using a Warhus camera and a sample to film distance of 5 cm. Cu radiation was used with a Ni filter ( $\lambda = 1.5405 \text{ \AA}$ ). Specimens were coated with Al powder for pattern calibration. Low-angle data were obtained at a distance of 29 cm, and the film was checked for shrinkage by use of preliminary marking of the film. The camera was evacuated to reduce air scatter after checking that specimens would be unaffected. Reflection intensities were visually estimated, and the film spacings were read on an illuminated film-measuring device.

Differential scanning calorimetry data were obtained using a Perkin-Elmer Model DSC-2. Runs were begun at room temperature and proceeded with a heating rate of 2.5 C/min. The calibration of the instrument was checked against the  $\alpha$  and  $\beta$  melting points of tristearin.

Many procedural variations led to a protocol for preparing specific forms of tristearin as follows: a portion of tristearin material was packed into the closed end of a Kimax

capillary tube having an inside diameter of 0.9 mm. The capillary triglyceride was placed in a water bath at temperatures greater than 85 C to insure completion of melting and then removed to quench in air to obtain the  $\alpha$  phase. The capillary was removed from the bath to a heating block at 55.0 C for 15-25 min to obtain the  $\beta'_2$  phase. Prolonged "setting" or "annealing" at 55 C resulted in carrying the triglyceride to the  $\beta$  phase. The fourth phase, the  $\beta'_1$  form, was obtained by immersing a capillary containing  $\beta'_2$  phase tristearin into a bath at 61-64 C. Duration of the heat treatment necessarily was 60-90 sec. Immersion of the sample for 2 min or longer converted the triglyceride to the  $\beta$ -state. Prolonged treatment of  $\beta'_2$  samples at temperatures less than 61 C failed to produce the  $\beta'_1$  phase. All 4 phases were stable at room temperature.

## RESULTS

### Raman Spectroscopy

The nature of Raman radiation allowed the solid samples to be studied directly in the form in which each was produced without further handling. The other analytical methods required removal of each glyceride sample from the capillary in which it was prepared.

Figure 1 presents the room-temperature Raman spectra of each phase. Spectral boundaries are from 875 to 1500  $\text{cm}^{-1}$  and from 1700 through 1750  $\text{cm}^{-1}$ . A comparison of the 2  $\beta'$  forms at -50 C is also given. The C-H stretching vibration region of 2800 through 3100  $\text{cm}^{-1}$  has been omitted, because no intensity or frequency changes were observed in this region other than those previously noted differentiating the  $\alpha$  and  $\beta'$  states against the  $\beta$  phase (9).

Vibrational observations peculiar to the individual phases of tristearin were taken within the 875-1750  $\text{cm}^{-1}$  Raman spectral region. In the  $\alpha$  and  $\beta'$  phases, the intensity of the 1063  $\text{cm}^{-1}$  vibration is greater than that of the 1130  $\text{cm}^{-1}$  band at room temperature. The spectrum of the  $\beta$  phase exhibits the reverse ratio for these 2 bands. The  $\alpha$  phase is distinguished from the  $\beta'$  forms in that the  $\alpha$  phase spectrum does not exhibit minor peaks at 922  $\text{cm}^{-1}$ , 1372  $\text{cm}^{-1}$ , 1731  $\text{cm}^{-1}$  and, most importantly, at 1421  $\text{cm}^{-1}$  at room temperature. This latter band was found characteristic only of the  $\beta'$  phases and serves further to differentiate the  $\beta'_1$  and  $\beta'_2$  states. The high-melting intermediate state,  $\beta'_1$ , exhibits a greater intensity for this vibration relative to the 1440  $\text{cm}^{-1}$  band than does its  $\beta'_2$  precursor. The 2  $\beta'$  phases were examined at ca. -50 C, a temperature at which the triglyceride hydrocarbon chain planes are considered to be in an all *trans* conformation (10). At the subzero temperature, the 1421  $\text{cm}^{-1}$  band exhibits improved resolution. Notable is the ratio of the intensity of the 1421  $\text{cm}^{-1}$  band to that of the 1463  $\text{cm}^{-1}$  band. For the  $\beta'_2$  phase, the ratio remains less than 1.0. In contrast, the intensity of the 1421  $\text{cm}^{-1}$  vibration in  $\beta'_1$  is significantly greater than the 1463  $\text{cm}^{-1}$  band at subzero temperatures resulting in a ratio greater than 1.0. The intensity ratio of  $I_{1421 \text{ cm}^{-1}}/I_{1440 \text{ cm}^{-1}}$  approximates 0.35 for  $\beta'_2$  and 0.52 for  $\beta'_1$  throughout the temperature range of -50 to +50 C. This observation provides an additional phase-specific property.

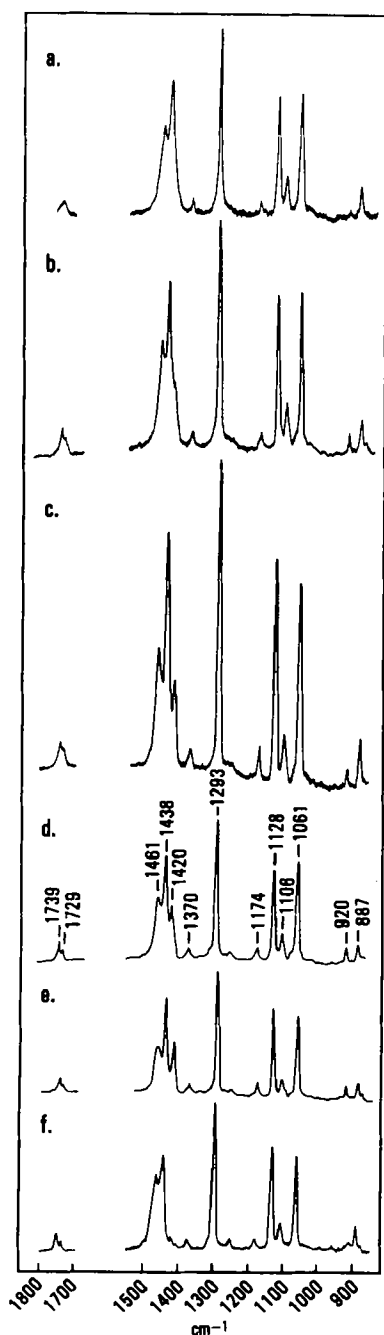


FIG. 1. Raman spectra of the 4 tristearin states at room temperatures and subzero temperatures. The phases represent (a)  $\alpha$ , (b)  $\beta'_1$ , (c)  $\beta'_2$  at  $-50$  C, (d)  $\beta'_1$ , (e)  $\beta'_1$  at  $-50$  C and (f)  $\beta$ .

#### Differential Scanning Calorimetry

The phase identity of each tristearin sample was checked by Raman spectroscopy before recording thermal behavior. Results of examinations by DSC are shown in Figure 2. The  $\alpha$  form does not exhibit any exothermic reaction other than its conversion to the  $\beta$  phase at  $55$  C as has been previously summarized (3). The DSC curves for the  $\beta'_1$  and  $\beta'_2$  forms are different in that the  $\beta'_2$  tristearin form exhibits a small but definite endothermic peak at  $61$  C. This gain of energy indicates the phase transformation to the  $\beta'_1$  state, which in turn converts to the  $\beta$  state at  $64$  C. Tristearin material placed initially in the  $\beta'_1$  phase does not exhibit an absorption of heat energy at  $61$  C but does convert to the  $\beta$  phase at  $64$  C. Samples entirely in the  $\beta$  phase show none of the above transitions.

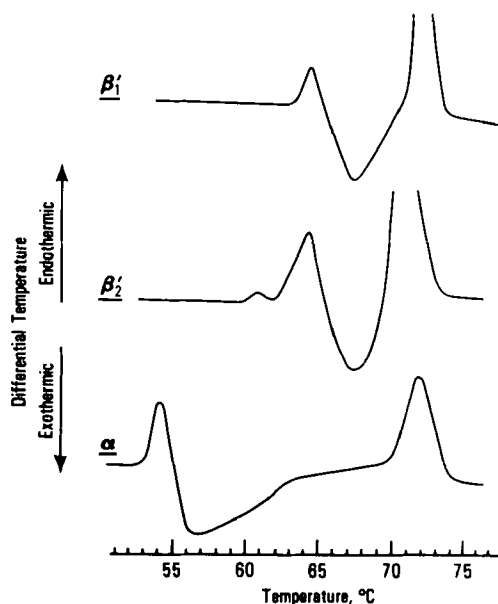


FIG. 2. DSC heating curves for tristearin phases showing phase transitions. The initial phase state of each curve is (a)  $\beta'_1$ , (b)  $\beta'_2$  and (c)  $\alpha$ .

#### X-Ray Diffraction

For X-ray diffraction analyses, thin slices of the triglyceride sample were removed, mounted and coated with Al for calibration. Powder diagram results for the  $\beta'_1$  phase are presented in Table I. The pattern for the  $\beta'_1$  state is almost identical to that for the  $\beta'_2$  state, which identifies with X-ray pattern results previously reported for the  $\beta'$  state of tristearin (1,3). Features that distinguish the 2 intermediate forms are: (a) a greater crystallinity in  $\beta'_1$ , evidenced by a sharper diffraction pattern, and (b) 2 distinct diffraction lines at  $4.1$  and  $4.3$  Å in  $\beta'_1$  as contrasted to a singular spacing at  $4.2$  Å in  $\beta'_2$ . Repeated efforts failed to provide evidence that the  $4.2$ -Å line for  $\beta'_2$  is a composite of the 2 diffraction lines witnessed for  $\beta'_1$ . Also in this regard, it is pertinent that Dafler (11) observed only the  $4.2$ -Å  $\beta'_2$ -type pattern in studying the  $\beta'$  to  $\beta$  transition in fully hydrogenated soybean oil. His experience with a known mixture (ca. 85% tristearin) tends to exclude

TABLE I

X-Ray Diffraction Data of the Tristearin  $\beta'_1$  State

Spacing (Å)	Intensity <sup>a</sup>	Indices
46.0 <sup>b</sup>	VVS <sup>b</sup>	001
15.3 <sup>b</sup>		
15.4	VS	003
11.2	W	004
9.23	M	005
7.71	WM	006
5.75	VW	008
5.39	VW	—
4.99	WM	—
4.72	VVW	—
4.51	W	—
4.27	VS	—
4.13	VS	—
3.99	M	—
3.79	VS	—
3.15	VVW	—

<sup>a</sup>Intensity scale: S = strong; M = medium; W = weak; WM = weak to medium; V = very.

<sup>b</sup>Low angle diffraction data.

impurities as a cause of the 2 distinct  $\beta'$  forms observed in this work.

## DISCUSSION

Results of the preparative method and the 3 instrumental investigative methods provide evidence for establishment of  $\beta'_1$  and  $\beta'_2$  as 2 independent phases of tristearin. The critical importance of a melting point in the preparative method is a compelling reason for distinguishing between 2 independent intermediate  $\beta'$  crystalline phases. If form conversion were occurring by annealing, temperatures just below 61 C should be expected to produce the observed behavior in little more time than the 1 min needed at and above 61 C. Such was not the case.

Differential scanning calorimetry results point also to a melting transition occurring at 61 C. The minor amount of energy involved suggests that the solid state change is subtle. This may explain why the phase change has not always been observed by previous investigators.

From the similarity of X-ray diffraction patterns, it is apparent that the  $\beta'_2$  unit cell dimensions and molecular structure are only slightly affected during the phase transition to  $\beta'_1$ . One must conclude therefore that the solid state change is but a subtle alteration in the intermolecular packing of the triglyceride molecules.

The improved crystalline state evident in the diffraction pattern for  $\beta'_1$  is important because it could enable collection of improved  $\beta'$  state X-ray diffraction data using an X-ray radiation counter equipped diffraction system. Data obtained in this manner should provide resolution of diffraction spacings and intensity measurements to allow for determination of the unit cell and subcell dimensions, as well as permitting solution of the unit cell hydrocarbon chain skeleton, if not the entire  $\beta'$  triglyceride. Such information is needed to clearly understand polymorphic transitions in fats. Examination at subzero temperatures, -50 C, would additionally simplify the structure solving by providing that all the hydrocarbon chain conformations are in the *trans* planar conformation.

The Raman spectral data yield no indication of any significant changes in band frequencies, yet the 1400 through 1500  $\text{cm}^{-1}$  region does contain the most distinguishing feature for discerning the 2  $\beta'$  phases, the 1421  $\text{cm}^{-1}$  band. The appearance of the 1421  $\text{cm}^{-1}$  band is not unprecedented, however, Larsson observed a similar result in the Raman study of simple lipids such as 1-monomyristin (9). He stated that the 1433  $\text{cm}^{-1}$  band indicated the presence of an orthorhombic or hexagonal packing structure. Absence of the band would indicate a triclinic or  $\beta$  structure. Yellin and Levin witnessed the appearance of a 1421  $\text{cm}^{-1}$  band in 1,2-diacyl phosphatidylcholine-water

gels (10). They showed that the band was a result of a  $\text{CH}_2$  methylene deformation mode and indicative of lateral chain interactions. Similar Raman observations have been found with 1,2-dilauroyl phosphatidylethanolamine (12), long-chain alkanes and polyethylene (13). The latter were studied by Boerio and Koenig who found that the 1418  $\text{cm}^{-1}$  band was characteristic of orthorhombic and monoclinic hydrocarbon chain packings, but it was not observable in triclinic or hexagonal packings in apparent contradiction to Larsson's correlation of the 1433  $\text{cm}^{-1}$  band with hexagonal packing. In any case, the presence or absence of a band at 1421  $\text{cm}^{-1}$  is a consequence of lateral interchain interactions.

The conclusions thus drawn in this study are that  $\beta'_1$  and  $\beta'_2$  are separate phase entities that differ in the lateral packing arrangement of the hydrocarbon chains. The  $\beta'_1$  phase is that state participating in the melting transition at 64 C, and the transition from the  $\beta'_2$  phase is only a minor thermodynamic change during transition to the  $\beta'_1$  state. As a result, the  $\beta'_1$  phase is believed to remain in an orthorhombic packing environment as found for  $\beta'_2$  (3). Although the overall molecular packing remains the same, the results indicate a finite restructuring of the chains or minor lateral packing rearrangement.

Although several investigative methods are necessary to provide sufficient evidence for establishment of the presence of mesophases, Raman spectroscopy appears to be the primary tool with which to probe further into the intricacies of lipid phase behavior, a physical process that is not yet fully disclosed, as this work indicates.

## REFERENCES

1. Lutton, E.S., JAOCS 27:276 (1950).
2. Malkin, T., Progress in the Chemistry of Fats and Other Lipids, Vol. 2, Academic Press, New York, NY 1954.
3. Chapman, D., The Structure of Lipids, John Wiley and Sons, New York, NY, 1965.
4. Hoerr, C.W., and F.R. Paulicka, JAOCS 45:793 (1968).
5. Larsson, K., Ark. Kemi 23:35 (1964).
6. Hagemann, J.W., W.H. Tallent and K.E. Kolb, JAOCS 49:118 (1972).
7. Lovegren, N.V., and M.S. Gray, Ibid. 55:310 (1978).
8. Chapman, G.M., E.E. Akehurst and W.B. Wright, Ibid. 48:824 (1971).
9. Larsson, K., Chem. Phys. Lipids 10:165 (1973).
10. Yellin, N., and I.W. Levin, Biochim. Biophys. Acta 489:177 (1977).
11. Dafler, J.R., JAOCS 54:249 (1977).
12. Mendelsohn, R., S. Sunder and H.J. Bernstein, Biochim. Biophys. Acta 413:329 (1975).
13. Boerio, F.J., and J.L. Koenig, J. Chem. Phys. 52:3425 (1970).

[Received August 11, 1981]